

A Stable Trinuclear Zinc Cluster Assembled from a Thiazolylazo Dye and Zinc Acetate: Preparation, Structural Characterization and Spectroscopic Studies

Guoqi Zhang,^[a] Shuangqing Wang,^[a] Quan Gan,^[a] Yongfang Zhang,^[a] Guoqiang Yang,^{*[a]} Jin Shi Ma,^[a] and Huijun Xu^[a]

Keywords: Azo compounds / Pi interactions / UV/Vis spectroscopy / Zinc

A thiazolylazo dye, 5-(diethylamino)-2-(2-thiazolylazo)phenol (HL), containing potential tridentate binding sites was synthesized in high yield and well characterized. In solution, the reaction of zinc acetate and the deprotonated ligand, L^- , results in the instantaneous formation of the supramolecular trinuclear species $[Zn_3L_2(OAc)_4]$ (**1**). UV/Vis and 1H NMR spectroscopic titration experiments in solution confirmed that the ligand and zinc salt interact spontaneously with each other and produce exclusively the polymetallic complex with the metal-to-ligand ratio of 3:2. The crystal structures of both the ligand and coordination complex are reported in this paper. The aromatic part of HL is planar and, significantly, the

intermolecular C–H $\cdots\pi$ hydrogen bonds and thiazole ring–S $\cdots\pi$ weak interactions observed here should be responsible for the orthorhombic space group $P2_12_12_1$. The structure of **1** reveals a linear trinuclear zinc cluster. The two L^- units are linked to three zinc atoms in an N_2O tridentate mode, and the four acetate anions are chelated to three metal centers as bridges to result in two pentacoordinate and one hexacoordinate zinc centers. The resulting bridging Zn1–Zn2–Zn1A array is linear by symmetry, with a nonbonding Zn \cdots Zn distance of 3.390 Å and a Zn1 \cdots Zn2 \cdots Zn1A angle of 180.0°. (© Wiley-VCH Verlag GmbH & Co. KGaA, 69451 Weinheim, Germany, 2005)

Introduction

Aromatic azo derivatives are widely used in the dyestuff industry, in analytical chemistry as acid-base, redox, and metallochromic indicators,^[1,2] and also, more recently, in the field of optical data storage and nonlinear optics.^[3,4] The structure of azo dyes has also attracted considerable attention over the years in view of their wide applicability as optical materials.^[5,6] While numerous publications have focused on the industrial applications of azo dyes, the structural characterization and studies of the metal-chelating properties of substituted azo compounds remain sparse in the literature.^[7–9]

Metal-chelating azo derivatives are considered to be some of the most promising optical materials.^[8,9] Coordination of transition metals to aromatic azo dyes not only results in a rich variety of supramolecular structures, but also in a significant enhancement of their nonlinearity, both of which are potentially useful in a wide range of optical devices. Hence, it is greatly promising to develop new functionalized azo-metal chelates. Goswami and co-workers have systematically studied metal coordination compounds of one class of pyridine-containing phenylazo ligands.^[10]

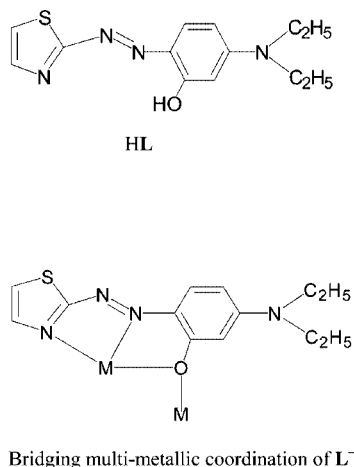
Divalent transition metals such as Zn^{II} , Cd^{II} , Hg^{II} , Ni^{II} , Pd^{II} , and Pt^{II} , or trivalent metals like Cr^{III} , In^{III} , etc., have been widely used to coordinate to the azo ligands. Accordingly, mononuclear or binuclear metallized azo complexes were obtained depending on the different nature of the metal ions. Their crystal structures, reactivity, and optical properties have also been investigated in detail.^[10]

Recently, we became interested in the investigation of a new class of azo derivative, namely 5-(diethylamino)-2-(2-thiazolylazo)phenol (HL), and its transition metal chelates (Scheme 1).^[8] The azo compound HL has several coordination sites and displays versatile chelating properties toward transition metal ions. The spectroscopic properties and third-order nonlinearity of certain transition metal complexes of HL have been investigated very recently. These results showed that the third-order nonlinearity is remarkably enhanced and size-tunable in nanoparticles of a nickel(II) complex of HL.^[8e]

Inspired by these interesting results on the nonlinearity and optical spectroscopic properties of this class of metallized thiazolylazo dyes as optical recording materials, we report here the synthetic procedure, solution properties, and structural characterization of the azo ligand HL and its zinc(II) complex. Both the ligand and complex display an ordered molecular arrangement in the solid state and significant intermolecular interactions are observed. The formation of the resultant trinuclear Zn^{II} cluster, as confirmed by both solution studies and X-ray diffraction analysis, is

[a] CAS Key Laboratory of Photochemistry, Institute of Chemistry, Chinese Academy of Sciences, Beijing 100080, P. R. China
E-mail: gqyang@iccas.ac.cn

Supporting information for this article is available on the WWW under <http://www.eurjic.org> or from the author.



Scheme 1. The structure of the azo ligand and its bridging multi-metallic binding mode.

the first example of an azo-based polymetallic cluster. Both compounds were characterized by microanalysis, TGA analysis, mass spectrometry, FT-IR, ^1H NMR, and UV/Vis spectroscopy, and single-crystal X-ray diffraction analysis.

Results and Discussion

Synthesis and Characterization

The thiazolylazo ligand HL was readily synthesized in high yield. The 2-aminothiazole precursor was diazotized with solid NaNO_2 in 85% phosphoric acid at $0-5^\circ\text{C}$ to give the diazonium salt, which was then added dropwise to the coupling component 3-diethylaminophenol in ethanol. After filtration, the azo dye was separated as a bright red solid. Block-like, deep-red crystals were obtained by slow evaporation of a MeOH/EtOH solution of the ligand. The azo dye is well soluble in common organic solvents like MeOH, EtOH, CH_2Cl_2 , CH_3CN , THF, etc. It is a potentially tridentate N,N,O-donor ligand for transition metal complexes, with the thiazolimine-N, azo-N, and phenoxo-O atoms providing the coordination sites, which can lead to versatile coordination models with different metal ions. Accordingly, the reaction of HL with zinc acetate hydrate resulted in the quantitative separation of an unusual trinuclear complex **1**. This needle-like complex is dark-red and also has excellent solubility in CH_2Cl_2 , CHCl_3 , and THF, etc. The structures of both the ligand and trinuclear zinc complex were confirmed by mass spectrometry, ^1H NMR, IR, and UV/Vis spectroscopy, and elemental analysis. X-ray diffraction analysis unambiguously confirmed the solid-state structures of both compounds.

UV/Vis Titration with Zn^{2+}

The formation of the zinc complex in solution was monitored by a UV/Vis titration experiment. Figure 1 shows the changes in the absorption spectra of the azo ligand HL upon increasing the concentration of Zn^{2+} in methanol.

The inset presents the plot of the absorbance at 540 nm as a function of the $[\text{Zn}^{2+}]/[\text{HL}]$ ratio. In methanol, the absorption spectrum of the free ligand exhibits a band with a maximum at 500 nm characteristic of the $\pi-\pi^*$ transition. The absorbance of this band decreases and a new band appears at around 540 nm upon increasing the $[\text{Zn}^{2+}]/[\text{HL}]$ ratio. An apparent isosbestic point appears at 512 nm, indicating the formation of a metal-ligand coordination compound. Furthermore, the inset shows a maximum at $[\text{metal}]/[\text{ligand}] = 1.5$, which indicates the formation of a 2:3 complex in solution.

X-ray Structural Analysis

An ORTEP view of HL, including the atomic numbering scheme, is shown in part a of Figure 2; selected bond lengths and angles are given in Table 1. The azo ligand crystallizes in the orthorhombic space group $P2_12_12_1$ with the Flack parameter refined to be 0.28(6), indicating the ligand crystallizes as a racemic twin. Overall, the conjugated aromatic part of the azo molecule is planar (part b, Figure 2); the dihedral angle of the two ring planes is only 4.0° . Interestingly, in the crystal packing of HL (part c, Figure 2), both intermolecular $\text{C-H}\cdots\pi$ hydrogen bonding and weak thiazole ring- $\text{S}\cdots\pi$ interactions are observed. While $\text{C-H}\cdots\pi$ hydrogen bonding is prevalent and also one of the most important intermolecular forces in the crystal packing of multi-aromatic systems,^[11] the thio $\cdots\pi$ weak interaction reported here is a new class of aromatic-aromatic interaction. It is well-known that the ability of the π -cloud of aromatic ring to interact with positively polarized atoms is not limited to $\text{C-H}\cdots\pi$ interactions,^[12] and electron-deficient cations can interact with aromatic systems, even biological macromolecules. In contrast, an interaction between electron-rich donors and/or anions with aromatic π -clouds is usually unexpected. A few papers are devoted to theoretical and experimental studies on this interaction.^[12] Hence, the observed interaction of an electron-rich thiazolyl S atom with a phenyl ring is reasonable, albeit unusual, on the basis of the similar reports.

The moderately strong $\text{C-H}\cdots\pi$ hydrogen bond has a separation of 3.082 Å for $\text{H}\cdots\pi$ -ring center and an angle of 146.3° for $\text{C-H}\cdots\pi$ -ring center,^[13] while the weak $\text{S}_{\text{thiazole}}\cdots\pi$ interaction has a short separation of 3.569 Å and a dihedral angle of 64.7° between the phenol and thiazole ring planes, comparable to the common distances of strong $\pi\cdots\pi$ interactions.^[14]

The neutral complex with a formula of $[\text{Zn}_3\text{L}_2(\text{OAc})_4]$ (**1**) was obtained by reaction of two equivalents of azo ligand with three equivalents of zinc(II) acetate hydrate in $\text{CH}_2\text{Cl}_2/\text{MeOH}$ solution, according to the results of the UV/Vis titration. Complex **1** crystallizes in the monoclinic space group $P2_1/c$. Its ORTEP structure is shown in Figure 3, in which two deprotonated ligand molecules L^- are linked with three zinc atoms, and two of three zinc atoms (Zn1 and Zn1A) are located in the thiazolylazo chelate moieties in a five-coordinate ZnN_2O_3 environment, with a thi-

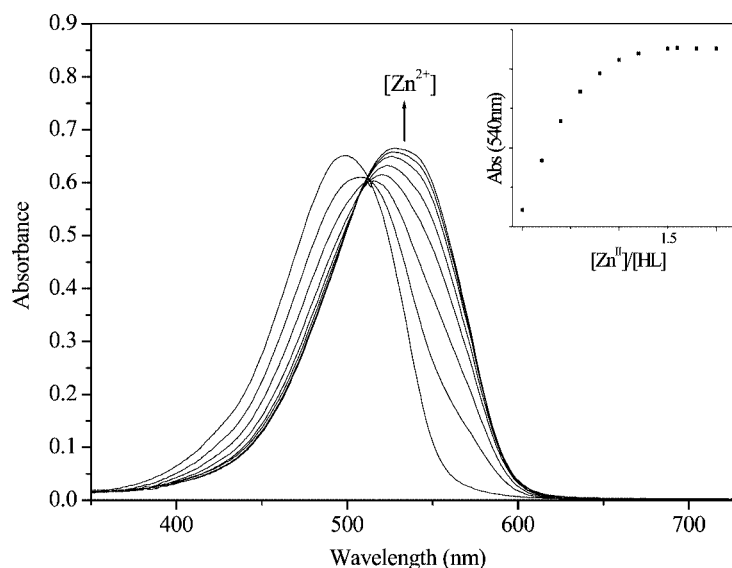


Figure 1. Change of absorption spectra of HL in methanol (1×10^{-5} M) upon addition of different concentrations of Zn^{2+} . Inset: plot of absorbance at 540 nm vs. the $[\text{Zn}^{2+}]/[\text{HL}]$ ratio.

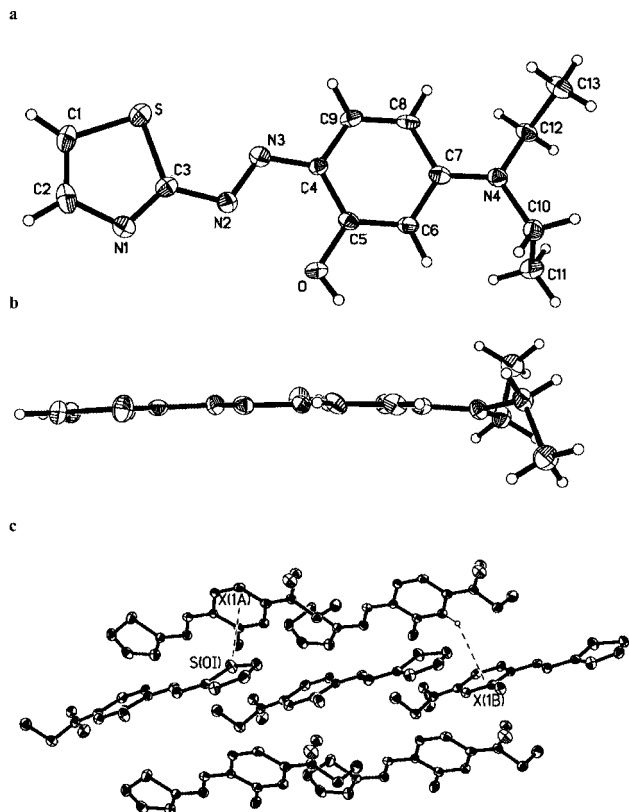


Figure 2. (a) ORTEP structure (30% probability level) and atom labeling scheme for azo ligand HL. (b) View along the plane of the azo moiety. (c) Crystal packing model showing the novel intermolecular $\text{S} \cdots \pi$ interaction and $\text{C-H} \cdots \pi$ hydrogen bonding.

azo nitrogen, an azo nitrogen, a phenoxo oxygen, and two oxygens from two acetate ions. The μ -phenoxo oxygen atoms (O1 and O1A), together with four acetate oxygen atoms, coordinate further to Zn2 at the inversion center to form a ZnO_6 octahedral geometry. Four μ -acetato ligands

Table 1. Selected bond lengths [\AA] and angles [$^\circ$] for HL and **1**.^[a]

HL			
S–C(1)	1.709(4)	S–C(3)	1.733(4)
O–C(5)	1.352(4)	N(1)–C(3)	1.303(4)
N(1)–C(2)	1.379(6)	N(2)–N(3)	1.303(4)
N(2)–C(3)	1.391(5)	N(3)–C(4)	1.351(4)
C(1)–S–C(3)	89.4(2)	C(3)–N(1)–C(2)	109.2(4)
N(3)–N(2)–C(3)	111.7(3)	N(2)–N(3)–C(4)	116.5(3)
C(7)–N(4)–C(12)	123.0(4)	C(7)–N(4)–C(10)	121.6(3)
C(12)–N(4)–C(10)	115.1(3)		
1			
Zn(1)–O(5)	1.946(2)	Zn(1)–O(3)	1.948(2)
Zn(1)–O(1)	2.094(2)	Zn(1)–N(3)	2.094(3)
Zn(1)–N(1)	2.162(3)	Zn(2)–O(1)	2.0753(19)
Zn(2)–O(1) ^{#1}	2.0753(19)	Zn(2)–O(4)	2.098(3)
Zn(2)–O(4) ^{#1}	2.098(3)	Zn(2)–O(2)	2.128(2)
Zn(2)–O(2) ^{#1}	2.128(2)		
O(5)–Zn(1)–N(3)	117.94(11)	O(3)–Zn(1)–N(3)	125.03(10)
O(1)–Zn(1)–N(3)	76.95(9)	O(5)–Zn(1)–N(1)	96.45(11)
O(3)–Zn(1)–N(1)	95.53(10)	O(1)–Zn(1)–N(1)	150.37(10)
N(3)–Zn(1)–N(1)	73.76(11)	O(5)–Zn(1)–O(3)	116.78(11)
O(5)–Zn(1)–O(1)	101.08(10)	O(3)–Zn(1)–O(1)	97.60(9)
O(1)–Zn(2)–O(2) ^{#1}	91.55(8)	O(1) ^{#1} –Zn(2)–O(2) ^{#1}	88.45(8)
O(4)–Zn(2)–O(2) ^{#1}	86.97(11)	O(2)–Zn(2)–O(2) ^{#1}	180.000(1)

[a] Symmetry transformations used to generate equivalent atoms: ^{#1} $-x + 1, -y, -z + 2$.

bind to three zinc centers (bridging Zn1–Zn2 and Zn1A–Zn2) and saturate the coordination numbers of zinc atoms, meaning that the whole charge of the complex is neutral. Thus, the resulting bridging Zn1–Zn2–Zn1A array is linear by symmetry. The nonbonding Zn \cdots Zn distance is 3.390 \AA , with a Zn1 \cdots Zn2 \cdots Zn1A angle of 180.0 $^\circ$, which indicates a weak interaction between the three zinc centers. The Zn–O bond lengths are in the range of 1.946(2)–2.128(2) \AA , and the Zn–N bond lengths are 2.094(3) \AA and 2.162 \AA , respectively (see Table 1), comparable to other known zinc complexes.^[15–17]

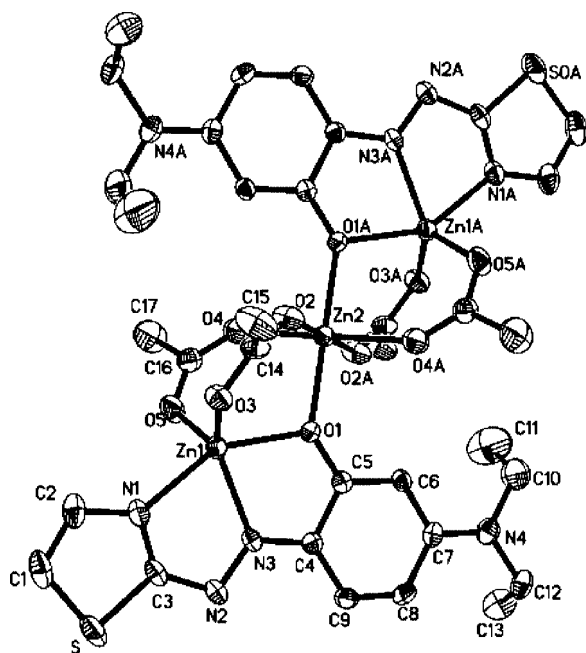


Figure 3. ORTEP structure (30% probability level) and atom-numbering scheme for trinuclear zinc cluster **1**. Hydrogen atoms have been omitted for clarity.

In addition, due to the good planarity and conjugation of the whole supramolecular complex, significant intermolecular $\pi\cdots\pi$ stacking interactions are observed in the crystal packing of **1** along the crystallographic *c* axis. (Figure 4) The aromatic planes of adjacent molecules are parallel, and the shortest C \cdots C and C \cdots N separations of $\pi\cdots\pi$ interactions are 3.426(4) Å and 3.455(4) Å, respectively, thus falling in the range of strong $\pi\cdots\pi$ interactions.^[14] It is worth mentioning that the reported metal complexes based on azo ligands usually adopt mono- or binuclear structures,^[10] therefore the trinuclear cluster structure depicted herein is surely the first example of an azo-based polynuclear Zn^{II} complex, although polynuclear cluster structures are not uncommon. Moreover, this observation may provide new references for designing other novel polynuclear metal complexes with special functional properties.

Spectroscopic Studies and Thermal Analysis

The infrared spectra (see Exp. Section) of ligand HL and complex **1** reveal the stretching vibration of the N=N band at 1431 and 1304 cm⁻¹. These values are indicative of the metal chelating behavior and are very similar to previous results.^[10d] The thiazole $\nu(\text{C}=\text{N})$ (1527 cm⁻¹) vibration appears as a very strong band which, upon complex formation, shifts to lower frequency (1501 cm⁻¹) with a reduction in its intensity.

The UV/Vis absorption spectra of both the free ligand HL and complex **1** were measured in various solvents. The $\pi\text{--}\pi^*$ transition band of HL is slightly solvent-dependent, the absorption maxima varied from 489 to 500 nm upon increasing the polarity of the solvent from ethyl acetate to

methanol. (Table 2) The spectra of two forms of the conjugated base and protonated salt of HL show a pronounced bathochromic shift, relative to that of HL in methanol, which was attributed to the formation of conjugated species. In contrast, the UV/Vis spectra of complex **1** show a remarkable solvent effect (see Supporting Information). In methanol, the spectrum exhibits a single peak at around 530 nm, while in other solvents like ethyl acetate, chloroform, and toluene etc. this single band splits into two or three fine peaks between 400 and 600 nm, indicating that this complex is very sensitive to the solvent environment.

In contrast, some salicylideneimine ligands usually form mononuclear or binuclear metal complexes depending on the substituents or the reaction conditions.^[17,18] As discussed previously, however, the $[\text{Zn}(\text{L}^-)]$ unit readily assembles spontaneously to give the stable 2:3 complex in excellent yield. The ¹H NMR titration experiment confirmed the cooperative formation and stability of the unique trinuclear complex $[\text{Zn}_3\text{L}_2(\text{OAc})_4]$ in solution. (see Supporting Information) The ¹H NMR spectra of the reaction were monitored by varying the amount of zinc(II) in CDCl₃/CD₃OD (1:1), and the results clearly indicated that a single species, $[\text{Zn}_3\text{L}_2(\text{OAc})_4]$, was formed very cooperatively upon the addition of a 1.5-fold amount of zinc(II).

The crystalline solid of complex **1** is stable up to 220 °C. The TGA curve exhibits an important weight loss from ca. 220 °C to 324 °C, assigned to the removal of four bridging acetate ions, with a weight decrease of 24.08% (calcd. 24.14%). Further heating leads to the degradation of the compound, which might be attributed to the elimination of azo ligand moieties (see Supporting Information).

Conclusions

In summary, we have synthesized and characterized a thiazolylazo dye and its zinc(II) complex. X-ray structure analysis showed the interesting intermolecular interactions, i.e. C–H $\cdots\pi$ hydrogen bonds and thiazole ring–S $\cdots\pi$ weak interactions, present in the crystal of HL, which are believed to play a crucial role in stabilizing the crystalline solid. A stable 2:3 complex was confirmed both in solution and in the solid state by UV/Vis, ¹H NMR, and FT-IR spectroscopy, elemental analysis, TGA measurements, and X-ray crystal diffraction. Spectroscopic studies showed that the formation of the trinuclear complex is highly efficient. The trinuclear zinc cluster complex obtained here is significant for building supramolecular arrays with novel optical properties. Further, the formation of the trinuclear complex from a multidentate azo-based chelate is interesting for the study of coordination-driven molecular assembly by introduction of various metal ions (transition metal or lanthanide ions), and also opens up new pathways for the design of more complicated and polynuclear metallosupramolecules by changing the appropriate substituent groups (and/or binding sites) on the azo ligand.

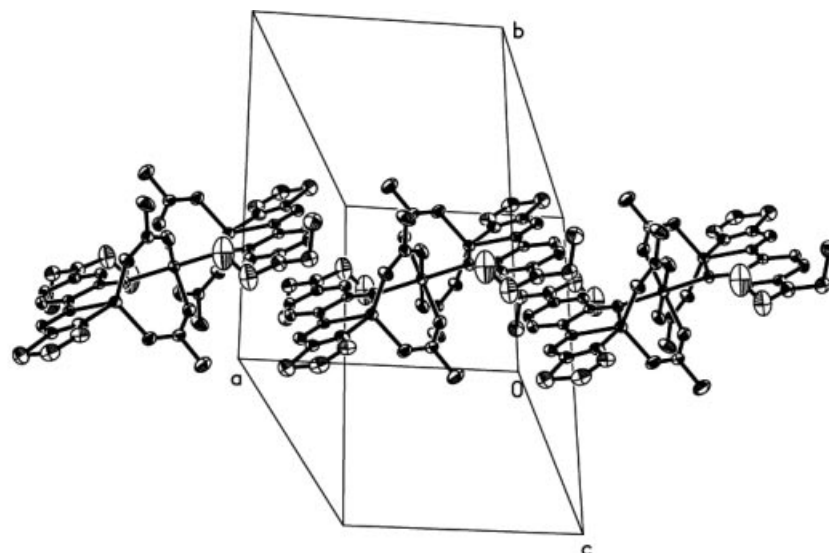


Figure 4. The crystal packing model of complex **1** along the crystallographic *c* axis showing the intermolecular $\pi\cdots\pi$ interaction.

Table 2. Spectroscopic data.

	Solvent	UV/Vis	Chemical shift in ppm (CDCl ₃)			IR
		λ_{\max} [nm] (ϵ [M ⁻¹ cm ⁻¹])	O–H	thiazolyl proton	aromatic proton	$\tilde{\nu}$ [cm ⁻¹]
HL	MeOH	500 (65456)	13.36(s)	7.78(d), 7.16(d)	7.53(d), 6.44(q) 6.15(d)	$\nu(\text{N}=\text{N})$ 1431 $\nu(\text{C}=\text{N})$ 1527
	CHCl ₃	496 (58581)				
	EtOAc	489 (62019)				
	C ₇ H ₈	491 (56261)				
L ⁻ [a] [H ₂ L]ClO ₄ 1	MeOH	508 (58374)		7.54(d), 7.21(d)	7.60(d), 6.47(q) 6.10(s)	$\nu(\text{N}=\text{N})$ 1304 $\nu(\text{C}=\text{N})$ 1501
	MeOH	540 (83294), 515 ^[b] (70404)				
	MeOH	530 (56898)				
	CHCl ₃	534 (43990), 563 ^[b] (42089)				
	EtOAc	520 (35120), 562 ^[b] (25697)				
	C ₇ H ₈	513 (31002), 566 ^[b] (23796)				

[a] The conjugated base, L⁻, was generated in situ by the addition of NEt₃ to a solution of HL in methanol. [b] Shoulder.

Experimental Section

Materials and Synthesis: All reagents and solvents for syntheses and analyses were of analytical grade and were used as received. Solvents for spectral measurements were purchased as spectrophotometric grade. 2-Aminothiazole, 3-diethylaminophenol and zinc acetate hydrate were purchased from Aldrich and used without further purification.

Synthesis of 5-(Diethylamino)-2-(2-thiazolylazo)phenol (HL). Diazotization of 2-Aminothiazole: 2-Aminothiazole (1.0 g, 0.01 mol) was dissolved in 15 mL of 85% phosphoric acid. The solution was cooled to 0–5 °C in an ice-brine bath and maintained at this temperature. Solid sodium nitrite (0.75 g, 0.011 mol, 10% excess) was added to the solution over 30 min and stirring was continued for 3 h, keeping the temperature in the range of 0–5 °C. Urea (50 mg) was then added to destroy the excess nitrous acid.

Coupling with 3-(Diethylamino)phenol: 3-(Diethylamino)phenol (1.65 g, 0.01 mol) was dissolved in 25 mL of ethanol and the solution was cooled to 0–5 °C in an ice-brine bath. The above diazonium solution was added portionwise to the coupling component, and maintained at 0–5 °C for 3 h. Then, 30 mL of water was added, stirring was continued for another 3 h, and the solution was allowed to stand overnight while the temperature rose spontaneously to room temperature. After filtration, 1.09 g of crude dye was obtained (yield 39.4%). The crude dye was purified by column

chromatography on neutral aluminum oxide using chloroform as eluent. Deep brown single crystals suitable for X-ray structure analysis were grown from a MeOH/EtOH solution of the azo dye. M.p.: 140–141 °C. MALDI-TOF-MS (C₁₃H₁₆N₄OS): m/z = 277 [M + 1]⁺, 299 [M + Na]⁺. FT-IR (KBr pellet): $\tilde{\nu}$ = 3410 cm⁻¹, 2972, 2361, 1636, 1527, 1474, 1431, 1336, 1272, 1181, 1137, 1008, 949, 807, 729, 683, 629. ¹H NMR (CDCl₃): δ = 1.26 (t, J = 7.14 Hz, 6 H), 3.47 (q, J = 7.14 Hz, 4 H), 6.15 (d, J = 2.61 Hz, 1 H), 6.44 (q, J = 9.30 Hz, 1 H), 7.16 (d, J = 3.33 Hz, 1 H), 7.53 (d, J = 9.30 Hz, 1 H), 7.78 (d, J = 3.33 Hz, 1 H), 13.36 (s, 1 H) ppm. C₁₃H₁₆N₄OS (276.1): calcd. C 56.50, H 5.84, N 20.27, S 11.60; found C 56.11, H 5.70, N 20.26, S 11.72.

Synthesis of Complex 1: The 5-(diethylamino)-2-(2-thiazolylazo)phenol dye (55.2 mg, 0.2 mmol) was dissolved in 10 mL of dichloromethane and a 5 mL methanol solution of zinc acetate hydrate (65.9 mg, 0.3 mmol) was added. The solution was stirred at room temperature for 2 h, then allowed to stand at 5 °C for two weeks. During this period dark-red needle-like crystals appeared and were collected by filtration, washed with diethyl ether, and dried under vacuum. Yield: 51.8 mg (53.0%). MALDI-TOF-MS: m/z = 859.21 [M – 2OAc]⁻, 741.1 [M – 4OAc]⁻. FT-IR (KBr pellet): $\tilde{\nu}$ = 2975 cm⁻¹, 2353, 1605, 1501, 1420, 1304, 1211, 1127, 1078, 1011, 949, 874, 826, 795, 665. ¹H NMR (CDCl₃): δ = 1.24 (t, J = 7.04 Hz, 12 H), 2.01 (s, 12 H), 3.50 (q, J = 7.08 Hz, 8 H), 6.10 (s, 2 H), 6.47 (q, J = 9.88 Hz, 2 H), 7.21 (d, J = 3.50 Hz, 2 H), 7.54 (d, J =

3.50 Hz, 2 H), 7.60 (d, $J = 9.81$ Hz, 2 H) ppm. $C_{34}H_{42}N_8O_{10}S_2Zn_3$ (978.0): calcd. C 41.54, H 4.31, N 11.40; found C 41.83, H 4.32, N 11.30.

Physical Measurements: Melting points were determined on a Yanaco MP-500 micro-melting point apparatus. MALDI-TOF MS measurements were carried out on a Bruker APEX II and KYKY-ZHP-5 spectrometer. FT-IR spectra were recorded on a BIO-RAD FT-165 IR spectrometer. Samples for C, H, N, and S analyses were dried under vacuum and the analysis were performed with a Carlo Erba-1106 elemental analyzer. Thermogravimetric analysis was performed with a Dupont 951 thermogravimetric analyzer under nitrogen atmosphere, with a heating rate of $10\text{ }^{\circ}\text{C min}^{-1}$. ^1H NMR spectra were measured with a Bruker dmX400 MHz NMR spectrometer at room temperature in CDCl_3 with tetramethylsilane as the internal reference. UV/Vis absorption spectra and solution titration measurement were obtained on a Hitachi UV-3010 absorption spectrophotometry. UV/Vis spectrophotometric titration experiments were carried out as follows: a solution of HL in MeOH (original concentration 1×10^{-5} M) was titrated directly in 10 mL volumetric flasks by successive addition of methanol solutions of zinc acetate hydrate. A concentrated $\text{Zn}(\text{OAc})_2 \cdot \text{H}_2\text{O}$ (0.01 M) solution was added in 2 to 20- μL aliquots using a microliter syringe. The absorption spectra were obtained by monitoring the spectra between 350 and 750 nm after transfer of the solution to a 1-cm quartz cell. The total volume change during the titration was negligible; the titration process was readily repeatable.

X-ray Crystallography: Crystals suitable for X-ray diffraction studies were obtained by solvent evaporation at $5\text{ }^{\circ}\text{C}$. Accurate unit-cell parameters were determined by a least-squares fit of 2θ values, measured for 200 strong reflections, and intensity data sets were measured on Rigaku Raxis Rapid IP diffractometer with Mo- K_α radiation ($\lambda = 0.71073\text{ \AA}$) at room temperature. The intensities were corrected for Lorentz and polarization effects, but no corrections for extinction were made. All structures were solved by direct methods. The non-hydrogen atoms were located in successive difference

Fourier synthesis. The final refinement was performed by full-matrix least-squares methods with anisotropic thermal parameters for non-hydrogen atoms on F^2 . The hydrogen atoms were added theoretically as riding on the concerned atoms. Crystallographic data and experimental details for structure analyses are summarized in Table 3. Selected bond lengths and angles data are listed in Table 1. CCDC-272172 (for HL) and -272173 (for **1**) contain the supplementary crystallographic data for this paper. These data can be obtained free of charge from The Cambridge Crystallographic Data Center via www.ccdc.cam.ac.uk/data_request/cif.

Supporting Information: Thermogravimetric analysis curve for complex **1**, absorption spectra for HL, L^- , and $[\text{H}_2\text{L}][\text{ClO}_4]$ in methanol, solvent-dependent absorption spectra for HL and **1**, and ^1H NMR titration spectra (Figures S1–S5).

Acknowledgments

We would like to express our sincere thanks to the Major State Basic Research Development Program of China (grant no. G2000078100) and the National Natural Science Foundation of China for the financial support (grant no. 50303019).

Table 3. Crystallographic data for compounds HL and **1**.

	HL	1
Empirical formula	$\text{C}_{13}\text{H}_{16}\text{N}_4\text{O}_5\text{S}$	$\text{C}_{17}\text{H}_{21}\text{N}_4\text{O}_5\text{SZn}_{1.5}$
Mol. mass	276.36	491.49
Color	Deep brown	Dark red
Crystal system	orthorhombic	monoclinic
Space group	$P2_12_12_1$	$P2_1/c$
T [K]	293(2)	293(2)
λ [Å]	0.71073	0.71073
a [Å]	7.6375(4)	10.0649(3)
b [Å]	8.8561(6)	15.9702(5)
c [Å]	19.9822(9)	14.0015(10)
α [°]	90.00	90.00
β [°]	90.00	110.1030(14)
γ [°]	90.00	90.00
V [Å ³]	1351.57(13)	2113.47(9)
Z	4	4
$F(000)$	584	1008
$\rho_{\text{calcd.}}$ [g cm ⁻³]	1.358	1.545
Crystal dimensions [mm ³]	$0.51 \times 0.11 \times 0.11$	$0.37 \times 0.22 \times 0.22$
Reflections collected	1785	4711
Unique reflections	793	2922
μ [mm ⁻¹]	0.237	1.849
$R^{\text{[a]}}$	0.0411	0.0408
$wR_2^{\text{[b]}}$	0.0697	0.0898

[a] $R = \Sigma(F_o - F_c)/\Sigma(F_o)$. [b] $wR_2 = \Sigma w[(F_o^2 - F_c^2)^2/\Sigma w(F_o^2)^3]^{1/2}$.

- [1] H. Rau, *Photochromism. Molecules and Systems* (Eds.: H. Dürr, H. Bouas-Laurent), Elsevier, Amsterdam, **1990**, chapter 4, p. 165.
- [2] H. Zollinger, *Color Chemistry, Syntheses, Properties and Applications of Organic Dyes and Pigments*, VCH Publishers, New York, **1987**, p. 92.
- [3] R. J. H. Clark, R. E. Hester, *Advances in Materials Science Spectroscopy*, John Wiley & Sons, New York, **1991**.
- [4] a) H. Bach, K. Anderle, Th. Fuhrmann, J. H. Wendorff, *J. Phys. Chem.* **1996**, *100*, 4135–4140; b) Z. Liu, C. Zhao, M. Tang, S. Cai, *J. Phys. Chem.* **1996**, *100*, 17337–17344; c) K. Taniike, T. Matsumoto, T. Sato, Y. Ozaki, K. Nakashima, K. Iriyama, *J. Phys. Chem.* **1996**, *100*, 15508–15516.
- [5] a) P. S. Ramanujam, S. Hvilsted, F. Andruzzi, *Appl. Phys. Lett.* **1993**, *62*, 1041–1043; b) G. J. Lee, D. Kim, M. Lee, *Appl. Opt.* **1995**, *34*, 138–143; c) P. S. Ramanujam, S. Hvilsted, I. Zebger, H. W. Siesler, *Macromol. Rapid Commun.* **1995**, *16*, 455–461; d) S. Hvilsted, F. Andruzzi, P. S. Ramanujam, *Opt. Lett.* **1992**, *17*, 1234–1236; e) I. Willner, S. Rubin, *Angew. Chem. Int. Ed. Engl.* **1996**, *35*, 367–385.
- [6] N. Biswas, S. Umapathy, *J. Phys. Chem. A* **2000**, *104*, 2734–2745.
- [7] a) M. Shivakumar, K. Pramanik, I. Bhattacharyya, A. Chakravorty, *Inorg. Chem.* **2000**, *39*, 4332–4338; b) A. C. G. Hotze, A. H. Velders, F. Ugozzoli, M. Biagini-Cingi, A. M. Manotti-Lanfredi, J. G. Haasnoot, J. Reedijk, *Inorg. Chem.* **2000**, *39*, 3838–3844; c) P. Gupta, R. J. Butcher, S. Bhattacharya, *Inorg. Chem.* **2003**, *42*, 5405–5411; d) A. Dogan, B. Sarkar, A. Klein, F. Lissner, T. Schleid, J. Fiedler, S. Zális, V. K. Jain, W. Kaim, *Inorg. Chem.* **2004**, *43*, 5973–5980.
- [8] a) S. Wang, S. Shen, H. Xu, D. Gu, J. Yin, X. Tang, *Dyes Pigm.* **1999**, *42*, 173–177; b) S. Wang, S. Shen, H. Xu, D. Gu, J. Yin, X. Dong, *Mater. Sci. Eng., B* **2001**, *79*, 45–48; c) S. Wang, S. Shen, H. Xu, *Dyes Pigm.* **2000**, *44*, 195–198; d) S. Wu, W. Qian, Z. Xia, Y. Zou, S. Wang, S. Shen, H. Xu, *Chem. Phys. Lett.* **2000**, *330*, 535–540; e) Z. Tian, W. Huang, D. Xiao, S. Wang, Y. Wu, Q. Gong, W. Yang, J. Yao, *Chem. Phys. Lett.* **2004**, *391*, 283–287.
- [9] a) P. Gopalan, H. K. Katz, D. J. McGee, C. Erben, T. Zielinski, D. Bousquet, D. Müller, J. Grazul, Y. Olsson, *J. Am. Chem. Soc.* **2004**, *126*, 1741–1747 and references cited therein; b) N. Ertan, P. Gürkan, *Dyes Pigm.* **1997**, *33*, 137–147.
- [10] a) K. K. Kamar, A. Saha, A. Castañeira, C.-H. Hung, S. Goswami, *Inorg. Chem.* **2002**, *41*, 4531–4538; b) S. Das, A. Saha, C.-H. Hung, G.-H. Lee, S.-M. Peng, S. Goswami, *Inorg. Chem.*

- 2003, 42, 198–204; c) S. Das, C.-H. Hung, S. Goswami, *Inorg. Chem.* **2003**, 42, 5153–5157; d) S. Das, C.-H. Hung, S. Goswami, *Inorg. Chem.* **2003**, 42, 8592–8597; e) K. K. Kamar, S. Das, C.-H. Hung, A. Castiñeiras, M. D. Kuz'min, C. Rillo, J. Bartolomé, S. Goswami, *Inorg. Chem.* **2003**, 42, 5367–5375.
- [11] a) M. A. Viswamitra, R. Radhakrishnan, J. Bandekar, G. R. Desiraju, *J. Am. Chem. Soc.* **1993**, 115, 4868–4869; b) W. L. Jorgensen, D. L. Severance, *J. Am. Chem. Soc.* **1990**, 112, 4768–4774; c) D. A. Evans, K. T. Chapman, D. T. Hung, A. T. Kawaguchi, *Angew. Chem. Int. Ed. Engl.* **1987**, 26, 1184–1186; d) D. Braga, F. Grepioni, E. Tedesco, *Organometallics* **1998**, 17, 2669–2672.
- [12] S. Demeshko, S. Dechert, F. Meyer, *J. Am. Chem. Soc.* **2004**, 126, 4508–4509 and references cited therein.
- [13] T. Steiner, *Angew. Chem. Int. Ed.* **2002**, 41, 48–76.
- [14] C. Janiak, *J. Chem. Soc., Dalton Trans.* **2000**, 3885–3896.
- [15] P. de Hoog, L. D. Pachón, P. Gamez, M. Lutz, A. L. Spek, J. Reedijk, *Dalton Trans.* **2004**, 17, 2614–2615.
- [16] J. Reglinski, S. Morris, D. E. Stevenson, *Polyhedron* **2002**, 21, 2175–2182.
- [17] S. Akine, T. Taniguchi, T. Nabeshima, *Inorg. Chem.* **2004**, 43, 6142–6144.
- [18] S. Mizukami, J. Houjou, Y. Nagawa, M. Kanesato, *Chem. Commun.* **2003**, 1148–1149.

Received: May 18, 2005

Published Online: September 8, 2005